Jurnal Kejuruteraan 36(2) 2024: 785–792
https://doi.org/10.17576/jkukm-2024-36(2)-35

Determination of Train Vehicle Speed using Fibre Bragg Grating Sensors for Railway Application

Nur Shufinah Suhaimi[a*], Meor Iqram Meor Ahmad[a], Mohd Zaki Nuawi[a], Mohd Hafizi Zohari[b], Ahmad Kamal Ariffin[a] & Aidie Zeid Muhammad Abdullah[d]

[a]*Department of Mechanical & Manufacturing Engineering, Faculty of Engineering and Built Environments, Universiti Kebangsaan Malaysia, 43600, UKM Bangi, Selangor, Malaysia*

[b]*Advanced Structural Integrity and Vibration Research (ASIVR), Faculty of Mechanical and Automotive Engineering Technology, Universiti Malaysia Pahang, 26600, Pekan, Pahang, Malaysia*

[c]*Rail Engineering Department, Track Network Maintenance Ampang Line, 5th Mile Jalan Ampang, 68000, Ampang, Selangor, Malaysia*

[*]Corresponding author: shufinahsuhaimi@gmail.com

Received 30 July 2022, Received in revised form 14 October 2023
Accepted 24 November 2023, Available online 30 March 2024

ABSTRACT

The average speed of the train can be determined by dividing the distance by the time taken to reach the targeted destination. Nevertheless, in the process of railroad travel, the pace of the train can either slow down or speed up depending on the circumstances. It is essential to conduct research into the speed of the railroad in particular conditions to ascertain what speed is appropriate for the railroad to run safely under certain conditions. This study is currently being conducted using Fibre Bragg Grating (FBG) sensors to determine the speed of the train at a specific point. Three different specific points are chosen. The speed is calculated by dividing the distance between two wheels on one bogie by the time between the two peaks representing the two wheels on one bogie. The train traveling between each point exhibits three different speed behaviours. It is currently found that the average speed at location 1 is 49.71 km/h, and the train is decelerating. At location 2, the average speed is 66.21 km/h, and the train moves at a constant speed. Lastly, at location 3, the average speed is 40.18 km/h, and the train is accelerating. In addition, the wavelength shifting signal can be utilized to count the train's axles. In this experiment, the train consists of 9 bogies with 18 sets of wheels. Therefore, this experiment demonstrates that FBG sensors can be used to determine the speed of the train at a certain location.

Keywords: Railway; Speed; FBG sensor; Axle count; Wavelength graph

INTRODUCTION

Since the 19th century, trains have been one of the earliest types of locomotive transportation. This kind of transportation is capable of carrying a substantial load over a great distance. Initially, trains are constructed to transport big loads to the coast for the purpose of exports (Nur Shufinah Suhaimi et al. 2022). On the other hand, in the modern world, trains are frequently utilized to transport passengers or individuals who want to travel for various reasons. Due to advances in technology, train travel has become both faster and more time and resource-efficient for passengers, allowing them to reach their destinations more quickly (Castillo-Mingorance et al. 2020). The train's speed can vary depending on its intended use or the amount of cargo it must transport. Commonly, the speed of trains in metropolitan areas that people use to travel to the city is slower than the speed of trains that travel very vast distances, such as from the city to the suburbs. From the city to the suburb, the train speed can reach up to 300 km/h compared to trains that travel in the city, where the speed can only reach 70 km/h (Feng et al. 2011; Zhou and Shen 2011). Not only that, but the speed of the train doesn't stay the same from one station to the next. It depends on when the train goes through the curve while going uphill and before it slows down to stop at the station or leaves the station. For the train to move safely on the rail, each section of track has a different speed. It's important to figure out how fast the train is going in different parts of the track.

The speed of the train can be determined by using sensors. Vehicle-based sensors are being used to determine the speed of the train (Ngigi et al. 2012). This type of sensor is implemented on any parts of the train that run on the track, such as accelerometers installed in the axle box of the train. Along with accelerometers, Fibre Bragg Grating (FBG) sensors are one of the possibilities to replace the traditional speed sensors currently employed to keep track of the train's speed. Numerous researchers are utilizing FBG sensors to analyze train metrics such as speed, axle counting, rail derailment, and wheel anomalies. This is possible because FBG sensors are unaffected by electromagnetic power and can be used in field experiments (N. S. Suhaimi et al. 2023). The research conducted by Lee et al. highlights the fact that FBG sensors have the potential to expand their further application. In addition to detecting the derailment of the rail, FBG sensors can also be used to count the number of axles, identify the train by recognizing the unique behavior of each wheel set, and determine the speed at which the train is traveling (Lee, Lee, and Ho 2004). The FBG sensors are being given serious consideration as the next possible measurement tools for rail track condition due to their resistance to electromagnetic interference, corrosion protection, ease of sensor multiplexing, and high resolution (Quan et al. 2014).

Within the scope of this study, FBG sensors were utilised to carry out speed measurements in three distinct places. The first place is where the train is making an attempt to come to a halt before it reaches the station. The second location is where the train is going at its highest speed, and the third location is where the train has just departed off the platform. The speed between these three locations is compared and analysed to determine, at each point, which speed behaviour begins to increase and which begins to decrease. This is done based on the result of the speed between these three locations. The time domain findings are displayed by the FBG sensors. The graph can be used to identify both the number of axle of the train and the number of wheels.

FBG WORKING PRINCIPAL

The FBG sensors has a Bragg Grating at its centre, and this grating is designed to accept light from a broadband light source as it passes through the grating. After that, a narrowband of light that has travelled will have its wavelength, which is known as the Bragg wavelength, reflected back (Hafizi et al. 2020). The Bragg wavelength can be expressed as:

$$\lambda_B = 2\eta_{eff}\Lambda \quad (1)$$

where λ_B, is the Bragg wavelength, while η_{eff} is the refractive index of the fibre and Λ is the gating period. Meanwhile the shift of the wavelength that influence by the axial strain and change of temperature can be expressed as:

$$\frac{\Delta\lambda_B}{\lambda_B} = (1 - Pe)\varepsilon + (\alpha + \xi)\Delta T \quad (2)$$

where $\Delta\lambda_B$is the shift of reflected Bragg wavelength, Pe is the photo-elastic coefficient, ε is the axial strain, α is the thermal expansion of coefficient, ξ is the thermos-optical coefficient and ΔT is change of temperature (Vorathin et al. 2018).

METHODOLOGY

The train that been chosen to conduct this research is in Kuala Lumpur on Ampang line section between Miharja

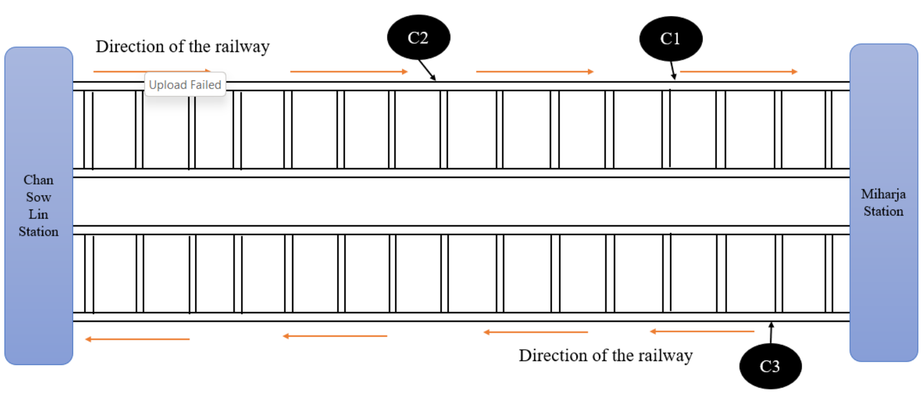

FIGURE 1. Illustration of 3 locations of the FBG sensor being placed on the rail track

station and Chan Sow Lin train station. When the train approaches the sensor position, the FBG sensors detect, and it is then utilised to calculate the train's speed as well as the number of axles. The FBG sensors are placed to three different locations. These three different locations have three different condition of train speed. First location is located 50 m from the platform which the train just departed from the platform and started to accelerate to move to the next platform. While the second location is located 600 m from the platform and in this location the train is at top speed. Finally in the third location is 120 m from the platform and the train is start to decelerated to stop to the platform. As in Figure 1, C1 represent location 1 the FBG sensor being place on the rail, while for C2 is for location 2 and C3 is for location 3.

The FBG sensors is patched using UV glue on the web surface of the rail. The FBG sensors is connected to the interrogation system by using long fibre cable. The speed of the train is analyzed from the wavelength signal from the FBG sensor. The route of the FBG sensors being installed on the rail as in Figure 2 below.

FIGURE 2. Fibre optic cable connected from sensor to the system on the platform

The installation of FBG sensors on the rail track as in Figure 3. The FBG sensors are installed on the web surface of the rail to avoid damages when the train move across the sensor. Then the FBG sensors is connected to the system that is placed on the platform as in Figure 4. Measured data from the FBG sensors is translated by the interrogation system and displayed on the computer as a wavelength signal.

FIGURE 3. FBG sensors are installed on the web section of the rail

FIGURE 4. Data acquisition system on the platform

The speed of the train can be determined by the wavelength shifting signal with the length between each of the train wheels. The length of section train as in Figure 5.

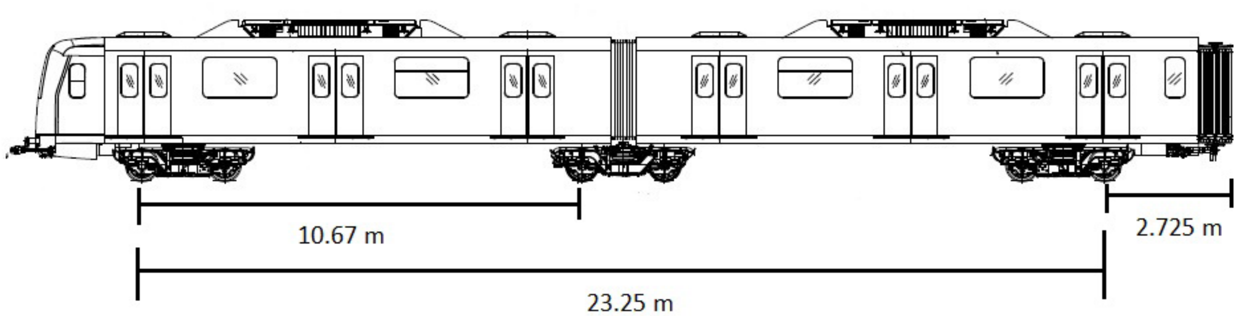

FIGURE 5. The length between wheels of the train

The train consists of 6 carriages with 9 bogies and 36 sets of wheels. Full illustration of the train can be seen as in Figure 6. The length between wheels no. 1 and no. 3 is 10.67 m. The length between wheels no. 1 and wheels no. 6 is 23.25m while for the total length from wheels no. 1 to wheels no. 18 is 80.65 m.

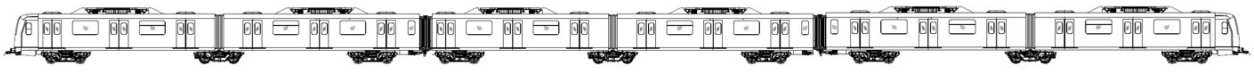

FIGURE 6. The illustration of the whole train

The speed of the train can be calculated by dividing the length between two sets of the wheels with the time taken of the two sets of the wheels. As the time can be taken form the wavelength signal from the FBG sensors between peak number 1 which represent the wheel no. one with peak number 3 which represent the wheel no. three. The length between wheel no. one and no. 3 already known. The speed can be calculated using formula as follows:

$$v = \frac{L}{t_{i+2} - t_i} \tag{3}$$

where v is the speed of the train, L is the length between two wheels set and t_i is the time for the specific no of wheel. To calculate the average speed of the whole train use the formula follows:

$$v_T = \frac{L_s}{t_f - t_o} \tag{4}$$

where L_s is the total length between wheel no. one to wheel no. 18, t_f is the time of the wheel no. 18 which the last peak and t_o is the time for wheel no. 1 which is the first peak.

RESULTS AND DISCUSSIONS

From the wavelength signal graph the number of wheels of the train can be determined (Ren et al. 2018). By counting the maximum movement of the FBG sensors or the highest point of the wavelength-shifting signal, the total number of wheels on the train can be found. The rail will momentarily distort or undergoes strain as the train passes over it. From Figure 7, the number of peak from the wavelength shifting signal graph is 18 peaks which represent 18 sets of wheels. These are briefly deformed by the force on the rail. The rail head experiences compression due to the shear weight of the train, whereas the rail foot experiences tension (Wei et al. 2010).

WHEEL-AXLE COUNT

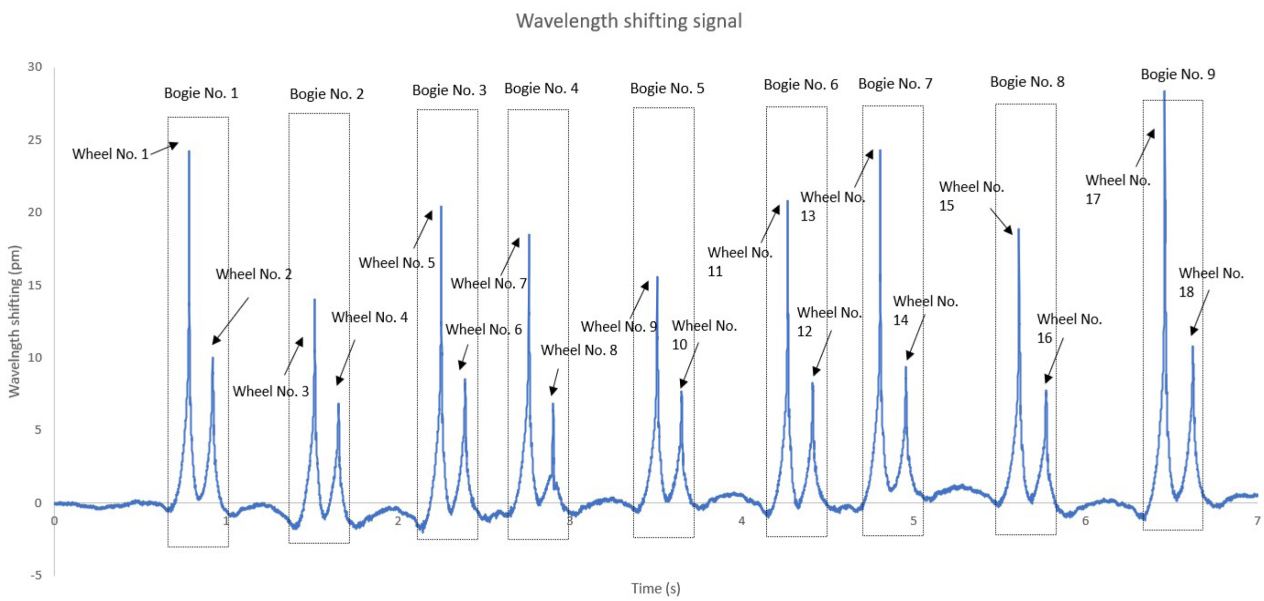

FIGURE 7. Wavelength shifting signal graph

SPEED OF THE TRAIN

There are three different locations with three different condition of speed of the train. The speed between each sets of wheels are calculated and tabulated as in Table 1. According to Track Network Maintenance Department, Rapid Rail, the average speed on location 1 is 50 km/h and train started to slow down. While the speed on location 2, the average top speed of the train would be 70 km/h and the last location which is location three, the average speed would be 35 km/h and the train is just started to speed up to go to the next platform. However by conducted this experiment the average speed of the train is sum up as Table 2. The average speed determined from the total length distance from the first wheel to the last wheel and the time taken to reach from the first wheel to the last wheel (Mennella et al. 2007).

TABLE 1. The speed of each wheel set of the train

Location	No. of wheel	Time (s)	Length between two set of wheels (m)	Speed (m/s)	Speed (km/h)
C1	1 & 3	0.73	10.67	14.59	52.53
	2 & 4	0.73	10.67	14.59	52.53
	3 & 5	0.74	10.67	14.51	52.25
	4 & 6	0.74	10.67	14.48	52.11
	5 & 7	0.51	7.36	14.40	51.85
	7 & 9	0.75	10.67	14.30	51.48
	8 & 10	0.75	10.67	14.28	51.39
	6 & 8	0.51	7.36	14.33	51.59
	9 & 11	0.76	10.67	14.05	50.56
	10 & 12	0.76	10.67	13.99	50.39
	11 & 13	0.54	7.36	13.69	49.30
	12 & 14	0.54	7.36	13.60	48.94
	13 & 15	0.81	10.67	13.19	47.49
	14 & 16	0.82	10.67	13.05	46.97
	15 & 17	0.85	10.67	12.58	45.29
	16 & 18	0.85	10.67	12.50	45.01
C2	1 & 3	0.58	10.67	18.35	66.07
	2 & 4	0.58	10.67	18.33	65.99
	3 & 5	0.58	10.67	18.33	65.99
	4 & 6	0.58	10.67	18.39	66.22
	5 & 7	0.40	7.36	18.41	66.26
	7 & 9	0.58	10.67	18.45	66.43
	8 & 10	0.58	10.67	18.41	66.29
	6 & 8	0.40	7.36	18.35	66.05
	9 & 11	0.58	10.67	18.37	66.14
	10 & 12	0.58	10.67	18.43	66.36
	11 & 13	0.40	7.36	18.41	66.26
	12 & 14	0.40	7.36	18.44	66.37
	13 & 15	0.58	10.67	18.50	66.59
	14 & 16	0.58	10.67	18.37	66.14
	15 & 17	0.58	10.67	18.41	66.29
	16 & 18	0.58	10.67	18.54	66.74
C3	1 & 3	1.06	10.67	10.03	36.09
	2 & 4	1.05	10.67	10.14	36.51
	3 & 5	1.01	10.67	10.58	38.07
	4 & 6	1.00	10.67	10.63	38.28
	5 & 7	0.68	7.36	10.88	39.15
	7 & 9	0.96	10.67	11.15	40.15
	8 & 10	0.95	10.67	11.22	40.40
	6 & 8	0.67	7.36	10.95	39.41
	9 & 11	0.93	10.67	11.47	41.29
	10 & 12	0.93	10.67	11.49	41.36
	11 & 13	0.63	7.36	11.62	41.82
	12 & 14	0.63	7.36	11.67	42.01
	13 & 15	0.90	10.67	11.81	42.50
	14 & 16	0.90	10.67	11.85	42.67
	15 & 17	0.89	10.67	12.01	43.23
	16 & 18	0.89	10.67	12.03	43.30

TABLE 2. Average speed of the train

Location	Actual vehicle speed, ν_R (km/h)	Average speed between each sets of wheel, ν_W (km/h)	Average speed of the whole train, ν_T (km/h)	Percentage difference of ν_W and ν_T (%)	Percentage difference of ν_R and ν_T (%)
C1	50	49.98	49.71	0.55	0.58
C2	70	66.26	66.21	0.08	5.56
C3	35	40.39	40.18	0.52	13.78

When compared to location one and location three, the speed at location two is significantly higher. As location two, the train was intended to be travelling at its maximum speed in order to arrive at the platform that was the following stop. According to Table 1, the speeds between each pair of wheels at each of the three distinct locations are not the same. This is because the train does not proceed at a constant speed in each spot where it stops. From location two, the speed is comparable to around 66 kilometres per hour for any number of wheel sets. This demonstrates that the train will neither speed up or slow down as it travels past this location in an effort to maintain a consistent speed throughout the journey. While for location one, the speed between the number of wheels is going from 52 kilometres per hour down to 45 kilometres per hour. This is because the train started to slow down or decelerate as it got closer to the station where it was going to stop. The speed is going up from 36 kilometres per hour to 43 kilometres per hour at location three. This indicates that the train is speeding up or moving more quickly now that it has just departed from the platform and is on its way to the next location.

As shown in Table 2, the average speed of the whole train is calculated by dividing the total length from 1 to 18 wheels by the time of the whole wheels pass the sensor. The average speed between each pair of wheels is the sum of the average speeds between each pair of wheels. The percentage difference of average speed between each sets of wheel and the average speed of the whole train is less than 1% percent for each location which means the calculated speed refer from the distance between wheels and refer to the total length of the whole bogie is almost the same. This value of speed is acceptable. The percentage difference of actual vehicle speed and the average speed of the whole train is less than 5% except for location three which hold 13%. This may be due to the actual vehicle speed given is the range speed of the location but not the exact speed for the specific point of location. Thus, potentially slightly different value between the speed that has been calculated to the speed that have been given from Rapid Rail Sdn Bhd.

CONCLUSION

There are three distinct locations, and each of these locations has three unique train passing scenarios. The first spot is when the train is slowing down as it approaches the station, the second place is when the train is travelling at its top speed, and the third place is when the train has just departed from the platform. The findings obtained from these three different places are compared to one another in order to determine the number of axles and the speed of the train at the significant place. According to the peak of the signal wavelength shifting that is being measured, the train has nine bogie axles and 18 wheels on each side. The axle count is based on the signal wavelength shifting.

When looking at the speed of the train as a whole, the first location displays a speed of 49.71 kilometres per hour, while the second location demonstrates a speed of 66.21 kilometres per hour, and the third location demonstrates a speed of 40.18 kilometres per hour. The train on second location has the highest speed since that's where the train is travelling at its top speed when you're in it. The speed behaviour is seen while comparing the speeds of each different number of wheels at each location. At the first site, the speed demonstrates behaviour consistent with deceleration; specifically, the speed decreases from the initial pair of wheels to the final pair of wheels. In the second position, the speed of the first pair of wheels and the speed of the last pair of wheels are virtually identical, which demonstrates that the train moves at a constant speed. Last but not least, the speed demonstrates an acceleration pattern at the third site, with the speed increasing from the first pair of wheels to the last pair of wheels as it moves to the third position. Because of this, the findings suggest that an FBG sensors can be used to detect train speed in addition to other metrics by utilizing a wavelength-shifting graph. This graph depicts the behaviour of a train as it travels through a sensor that has been installed at a particular place. In this field experiment, the study successfully accomplished its goals of utilizing FBG sensors to ascertain the speed of trains at specific locations. Nevertheless, the results of this experiment also suggest a promising avenue for further investigation, focusing on the correlation between train speed and the strain experienced by the rail track. Given that FBG sensors can be used for strain detection, delving into this aspect could yield valuable insights. By analyzing the strain patterns exhibited by the running rail track, a multitude of mechanical inquiries can be pursued, including an exploration into the impacts of fatigue and creep phenomena on the rail's integrity.

ACKNOWLEDGENT

The research has been funded by the Ministry of Higher Education (MOHE) Malaysia under the Fundamental Research Grant Scheme with grant number FRGS/1/2020/TK02/UKM/03/1.

DECLARATION OF COMPETING INTEREST

None

REFERENCES

Castillo-Mingorance, Juan Manuel, Miguel Sol-Sánchez, Fernando Moreno-Navarro, and María Carmen Rubio-Gámez. 2020. "A Critical Review of Sensors for the Continuous Monitoring of Smart and Sustainable Railway Infrastructures." *Sustainability (Switzerland)* 12 (22): 1–20. https://doi.org/10.3390/su12229428.

"Development of Temperature-Insensitive Fibre Bragg Grating Pressure Transducer Development of Temperature-Insensitive Fibre Bragg Grating Pressure Transducer." 2020. *Z.M. Hafizi, A.M. Aizuddin, E. Vorathin*. https://doi.org/10.1088/1757-899X/788/1/012088.

Feng, Xuesong, Baohua Mao, Xujie Feng, and Jia Feng. 2011. "Study on the Maximum Operation Speeds of Metro Trains for Energy Saving as Well as Transport Efficiency Improvement." *Energy* 36 (11): 6577–82. https://doi.org/10.1016/j.energy.2011.09.004.

Lee, KY, KK Lee, and SL Ho. 2004. "Exploration of Using FBG Sensor for Derailment Detector." *WSEAS Transactions Topics Systems* 3 (6): 2433–2439.

Mennella, F, A Laudati, M Esposito, A Cusano, and A Cutolo. 2007. "Railway Monitoring and Train Tracking by Fiber Bragg Grating Sensors" 6619: 7–10. https://doi.org/10.1117/12.738593.

Ngigi, R. W., C. Pislaru, A. Ball, and F. Gu. 2012. "Modern Techniques for Condition Monitoring of Railway Vehicle Dynamics." *Journal of Physics: Conference Series* 364 (1). https://doi.org/10.1088/1742-6596/364/1/012016.

Quan, Yu, Dawei He, Yongsheng Wang, and Pengfei Wang. 2014. "Axle Counter for High-Speed Railway Based on Fibre Bragg Grating Sensor and Algorithm Optimization for Peak Searching." *7th International Symposium on Advanced Optical Manufacturing and Testing Technologies: Smart Structures and Materials for Manufacturing and Testing* 9285: 92850D. https://doi.org/10.1117/12.2068055.

Ren, Liang, Tangzheng Feng, Michael Ho, Tao Jiang, and Gangbing Song. 2018. "A Smart 'Shear Sensing' Bolt Based on FBG Sensors." *Measurement: Journal of the International Measurement Confederation* 122 (March): 240–46. https://doi.org/10.1016/j.measurement.2018.03.026.

Suhaimi, N. S., M. I.M. Ahmad, M. Z. Nuawi, A. K. Ariffin, and A. Z.M. Abdullah. 2023. "Structural Condition Assessment Based Strain-Stress Behaviour for Railway Welded Rail Joint Using Rosette Fibre Bragg Grating Optical Sensor." *Results in Engineering* 19 (July): 101300. https://doi.org/10.1016/j.rineng.2023.101300.

Suhaimi, Nur Shufinah, Meor Iqram, Meor Ahmad, Mohd Zaki Nuawi, Ahmad Kamal, and Nur Azam Abdullah. 2022. "A Review on Modes of Failure of Rail Tracks Structure in Railway Transportation." *ASEAN Journal of Engineering and Technology* 2 (1): 1–7. https://doi.org/10.26666/rmp.ajte.2022.1.2.

Vorathin, E., Z. M. Hafizi, S. A.Che Ghani, J. P. Siregar, and K. S. Lim. 2018. "FBGs Real-Time Impact Damage Monitoring System of GFRP Beam Based on CC-LSL Algorithm." *International Journal of Structural Stability and Dynamics* 18 (5): 1–23. https://doi.org/10.1142/S021945541850075X

Wei, Chu Liang, Chun Cheung Lai, Shun Yee Liu, W. H. Chung, T. K. Ho, Hwa Yaw Tam, S. L. Ho, A. McCusker, J. Kam, and K. Y. Lee. 2010. "A Fiber Bragg Grating Sensor System for Train Axle Counting." *IEEE Sensors Journal* 10 (12): 1905–12. https://doi.org/10.1109/JSEN.2010.2049199.

Zhou, Li, and Zhiyun Shen. 2011. "Progress in High-Speed Train Technology around the World." *Journal of Modern Transportation* 19 (1): 1–6. https://doi.org/10.1007/bf03325733.